

## Surface second-harmonic generation from metal island films and microlithographic structures

A. Wokaun, J. G. Bergman, J. P. Heritage, A. M. Glass, P. F. Liao, and D. H. Olson

*Bell Laboratories, Holmdel, New Jersey 07733*

(Received 20 January 1981)

Enhanced second-harmonic generation is observed from silver and gold island films, and from regular arrays of Ag particles produced by microlithographic techniques. Enhancements are interpreted in terms of an electromagnetic model involving localized surface-plasma oscillations. The regular arrays allow the separation of fundamental and second-harmonic beams by a novel grating effect.

### I. INTRODUCTION

The enhancement of surface phenomena due to microscopic surface roughness has been the subject of numerous investigations during recent years. Examples are surface-enhanced Raman scattering (SERS)<sup>1,2</sup> from metal surfaces roughened by various techniques,<sup>3-8</sup> and enhanced luminescence from dye monolayers spun on silver and gold island films.<sup>9</sup> An electromagnetic model<sup>10-14</sup> explains these enhancements as being due to amplification of incident and reradiated fields by plasmon resonances on the surface. Surface second-harmonic generation (SHG) can also be enhanced by the same mechanism, as has recently been demonstrated by Chen *et al.*<sup>15</sup> on electrochemically roughened bulk silver.

The present study reports SHG from Ag and Au island films of continuously varying thickness, and from Ag particles on a lithographically produced microstructure. For the island films, we explicitly demonstrate the dependence of the SHG enhancement on the resonant excitation of a localized surface plasmon. This result is supported by measurements of the optical properties, and of SERS from CN adsorbed on the films. The Ag particles on the microstructures were specifically designed to resonate the second-harmonic (SH) frequency. The regularity of the employed array results in a novel grating effect, and a Gaussian beam of SH light well separated from the incident and reflected fundamental beams is created.

### II. ENHANCED SECOND-HARMONIC GENERATION FROM SURFACES

SHG on planar surfaces<sup>16</sup> has been the subject of numerous investigations in the past. The sym-

metry-breaking presence of the surface<sup>17-20</sup> is a necessary requirement for media with inversion symmetry to generate a field at the SH frequency. Theoretical accounts<sup>21-24</sup> of SHG on metal surfaces have weighted the relative contributions of "volume-type" terms, due to conduction and core electrons next to the boundary, and of "surface-type" quadrupolar terms, caused by the gradient of the electric field at the interface.

The enhancement of SHG by granular structures on the surface is in several aspects related to SERS.<sup>1,2</sup> The SH light is created in a thin surface layer of the metal particle, while the enhanced Raman signal arises from layers of scatterers overcoating the particle. The mechanism underlying both types of enhancement is the presence of a modified field<sup>7,8,10-14</sup>  $E_{in}$  inside of particles (small compared to the wavelength) in an electromagnetic field  $E_0$ ,

$$E_{in} = \frac{1}{1 + [\epsilon(\omega) - 1](A + B)} E_0 = f(\omega) E_0, \quad (1)$$

where  $\epsilon(\omega)$  is the complex dielectric function of the metal and  $A$  is a depolarization factor<sup>25</sup> depending on the shape of the particle. The constant  $B = v \sum_{j \neq i}^N \gamma_{ij} r_{ij}^{-3} / 4\pi$  accounts for the dipolar interactions among particles. Here  $v$  is the volume of a particle, and  $\gamma_{ij} = 1 - 3 \cos^2 \theta_{ij}$ , with  $\theta_{ij}$  the angle between  $\vec{E}_0$  and the interparticle vector  $\vec{r}_{ij}$ . Equation (1) defines the local field enhancement factor<sup>7</sup>  $f(\omega)$  for small particles in the long-wavelength limit. Resonant amplification of the internal field occurs if shape, packing density, and frequency match to fulfill the condition  $\epsilon(\omega) \approx 1 - 1/(A + B)$ .

For SERS, the adsorbed molecules are polarized by the amplified fields just outside the surface. They are related to  $E_{in}$  [Eq. (1)] by the dielectric

function; e.g., for a spheroid excited along the major axis, a molecule at the tip of the spheroid experiences a field  $\epsilon(\omega)E_{\text{in}}$ . The scattered field produced by the vibrating molecular dipole is then amplified a second time by the metal particle, leading to a Raman polarization,<sup>8,10-14</sup>

$$P^{(2)}(\omega_R) \propto [\epsilon(\omega_R) - 1]f(\omega_R)\alpha_R[\epsilon(\omega_0) - 1] \times f(\omega_0)E_0, \quad (2)$$

where  $\alpha_R$  is the Raman cross section. In contrast, for an  $n$ th-order nonlinear process occurring in the surface layer of the particle itself, the polarization is given by

$$P^{(n)} \left[ \sum_{i=1}^n \omega_i \right] = \left[ \epsilon \left[ \sum_{i=1}^n \omega_i \right] - 1 \right] f \left[ \sum_{i=1}^n \omega_i \right] \times \chi^{(n)} \prod_{i=1}^n \frac{[\epsilon(\omega_i) - 1]f(\omega_i)E_i}{\epsilon(\omega_i)}.$$

Factors  $\epsilon(\omega_i)$  appear in the denominator for the incident frequencies because the enhanced fields inside the metal are relevant; these factors tend to reduce the enhancement since  $|\epsilon(\omega)|$  is large in the visible spectrum for the metals of interest. The effective nonlinear susceptibility for small particles  $\chi^{(n)}$  is shape dependent (in general, a tensor) and cannot be related in a straightforward fashion to the properties of a perfect planar surface. For an isolated sphere of dimensions much smaller than the excitation wavelengths,  $\chi^{(n)} = 0$  by symmetry for even  $n$ . In our experiments,  $\chi^{(2)} \neq 0$  due to the inherent asymmetry of particles affixed to a substrate of high refractive index (sapphire).

Note that as in the case of SERS, both the input fields at frequencies  $\omega_i$  and the reradiated field at  $\omega = \sum_{i=1}^n \omega_i$  can be enhanced according to Eq. (3). For SHG, the large difference in frequency of the input and output fields makes their simultaneous enhancement more difficult. We have designed, in two different ways, particles on surfaces to resonate either the fundamental  $\omega_1$  or the SH frequency  $2\omega_1$  in Eq. (3). Firstly, we use vacuum-deposited Ag and Au island films<sup>7</sup> of varying thickness to achieve a continuous variation of the dielectric properties (due to changing particle size and density). For Ag, the SH intensity maximizes at a mass thickness appropriate to excite a particle plasmon at the SH frequency. For the Au film, no such resonance exists, and the SHG maximum occurs for a mass thickness supporting a particle plasmon at the fundamental

wavelength (1.06  $\mu\text{m}$ ). Secondly, we employ an array of Ag particles on a lithographically prepared microstructure which has been specifically designed<sup>8</sup> for a particle plasmon resonance at 0.53  $\mu\text{m}$ .

Samples were excited by a train of 140-ps pulses at  $\lambda = 1.06 \mu\text{m}$  from a mode-locked cw Nd:YAG (yttrium aluminum garnet) laser with a pulse rate of 100 MHz. This mode of operation allows one to deliver the highest peak power compatible with thermal conductivity, and to increase the sensitivity by chopping and phase-sensitive detection. (Earlier attempts to use  $Q$ -switched lasers had failed due to burning problems.) A beam of 1.2 W average power was focused onto a 22- $\mu\text{m}$ -diameter spot on the sample after blocking any visible light from the flashlamps. The second-harmonic light passed through a narrow-band filter followed by a color filter blocking the fundamental and was detected with a photomultiplier.

### III. EXPERIMENTS ON METAL ISLAND FILMS

Metal island films were prepared by evaporating, at a rate of 3–4  $\text{\AA}/\text{s}$ , Ag or Au onto sapphire substrates in a vacuum of  $10^{-6}$  Torr. Sapphire was preferred over glass or quartz because of its higher thermal conductivity; films on glass or quartz substrates were damaged at the same power levels. A “wedge” of continuously varying thickness<sup>7</sup> from 0 to  $\sim 200 \text{\AA}$  was produced by moving a shutter across the surface during evaporation.

#### A. Second-harmonic generation

Figure 1(a) shows the SH intensity for an Ag island film as a function of mass thickness  $d_m = m/\rho$ , where  $m$  is the mass deposited per unit area and  $\rho$  is the bulk density. The trace was obtained by translating an Ag “wedge” in the focal plane of the fundamental beam. The SH signal shows the following characteristic features. Starting from a true zero at  $d_m = 0$ , the intensity reaches a maximum at  $d_m \approx 36 \text{\AA}$ , drops close to zero at  $d_m \approx 65 \text{\AA}$ , and then reaches a plateau corresponding to  $\sim 10\%$  of the peak value for  $d_m \geq 100 \text{\AA}$ . The uncertainty in the mass thicknesses quoted throughout the text is typically  $\pm 5 \text{\AA}$ .

Quadratic dependence of the signal on input power was verified. The polarization behavior is in agreement with earlier measurements.<sup>17,23</sup> The SH intensity from a  $p$ -polarized fundamental beam was

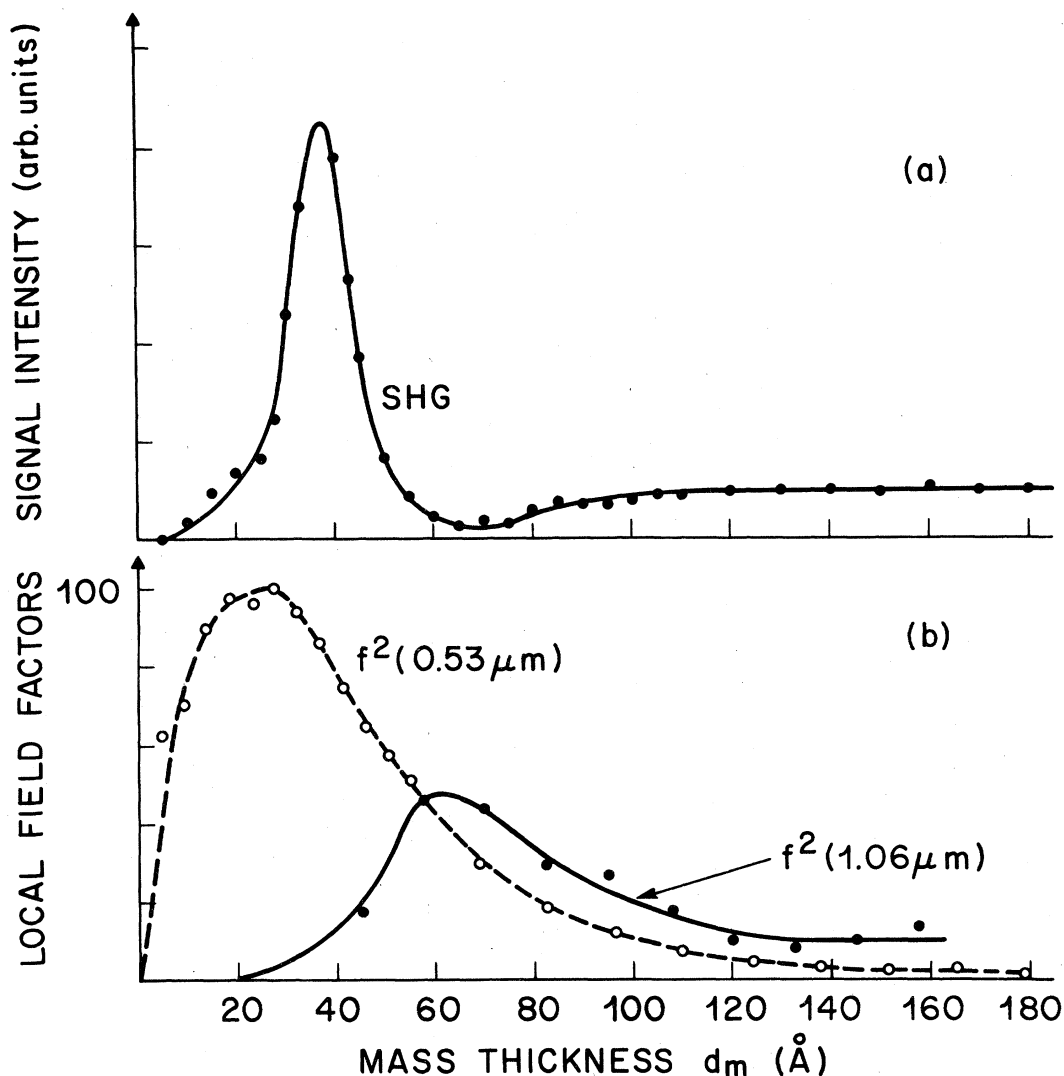


FIG. 1. SHG from Ag island films as a function of mass thickness  $d_m$  (see text). (a) Second-harmonic intensity excited at  $1.06 \mu m$ . (b) Local field enhancement factors  $|f|^2$  at  $1.06 \mu m$  (solid circles) and  $0.53 \mu m$  (open circles).

stronger by a factor of  $\geq 10$  compared to  $s$ -polarized excitation. The reradiated SH wave was  $p$ -polarized independent of the input, the perpendicular component being suppressed by a factor of  $\geq 10$ . An angle of incidence close to  $50^\circ$  and  $p$ -polarized excitation were used for all measurements reported below.

Our detection sensitivity was calibrated against the SH intensity from one coherence length of a standard quartz sample, observed under identical experimental conditions. Using the known nonlinear susceptibility<sup>26</sup> one obtains a ratio of  $(I_{2\omega}/I_\omega^2)_{\text{quartz}} = 6.3 \times 10^{-15} \text{ cm}^2 \text{ W}^{-1}$ . The peak signal from Ag films corresponds to  $4 \times 10^{-4}$  of the quartz signal, or  $(I_{2\omega}/I_\omega^2)_{\text{Ag}} = 2.5 \times 10^{-18}$

$\text{cm}^2 \text{ W}^{-1}$ . Comparing this number with the SH conversion efficiency reported by Bloembergen<sup>18,23</sup> ( $I_{2\omega}/I_\omega^2 = 2.4 \times 10^{-21} \text{ cm}^2 \text{ W}^{-1}$  when converted to the same units) and related measurements of Wang and Duminski,<sup>20</sup> we calculate a peak surface SH enhancement of  $10^3$ .

The determination of SHG efficiencies is subject to considerable uncertainties. Signals have been reported both to decrease<sup>27</sup> and to increase<sup>24</sup> due to adsorption of contaminants onto a fresh Ag surface. To ensure that our signals are not due to surface contamination, we have exposed our samples to HCN vapor, whereby a monolayer<sup>4</sup> of CN is chemisorbed by the silver, but were not able to detect a significant change in the SH intensity. Furthermore,

we performed experiments on polished Ag bars, with part of the surface electrochemically roughened<sup>4</sup> in a 0.2M KF–0.01M KCN solution. The SH signal from the roughened surface corresponded in magnitude to the peak signal from Ag island films, while the polished parts of the bars yielded 10–50 times smaller signals. These two tests give us confidence that the observed SHG signals are due to Ag particles, not due to surface contaminants or the supporting substrate.

Corresponding results for Au island films are shown in Fig. 2(a). The SH intensity shows a sharp peak at  $d_m \approx 40 \text{ \AA}$ , drops close to zero for

$d_m \approx 65 \text{ \AA}$ , and again reaches a plateau for  $d_m \geq 120 \text{ \AA}$ . The peak value ( $8 \times 10^{-19} \text{ cm}^2 \text{ W}^{-1}$ ) reached in the area of isolated islands is smaller than for Ag, and the SH generation on the thick Au film is almost by a factor of 2 larger than that of the islands.

#### B. Optical properties and SERS experiments

In order to understand the observed dependences on mass thickness, we have determined the relevant

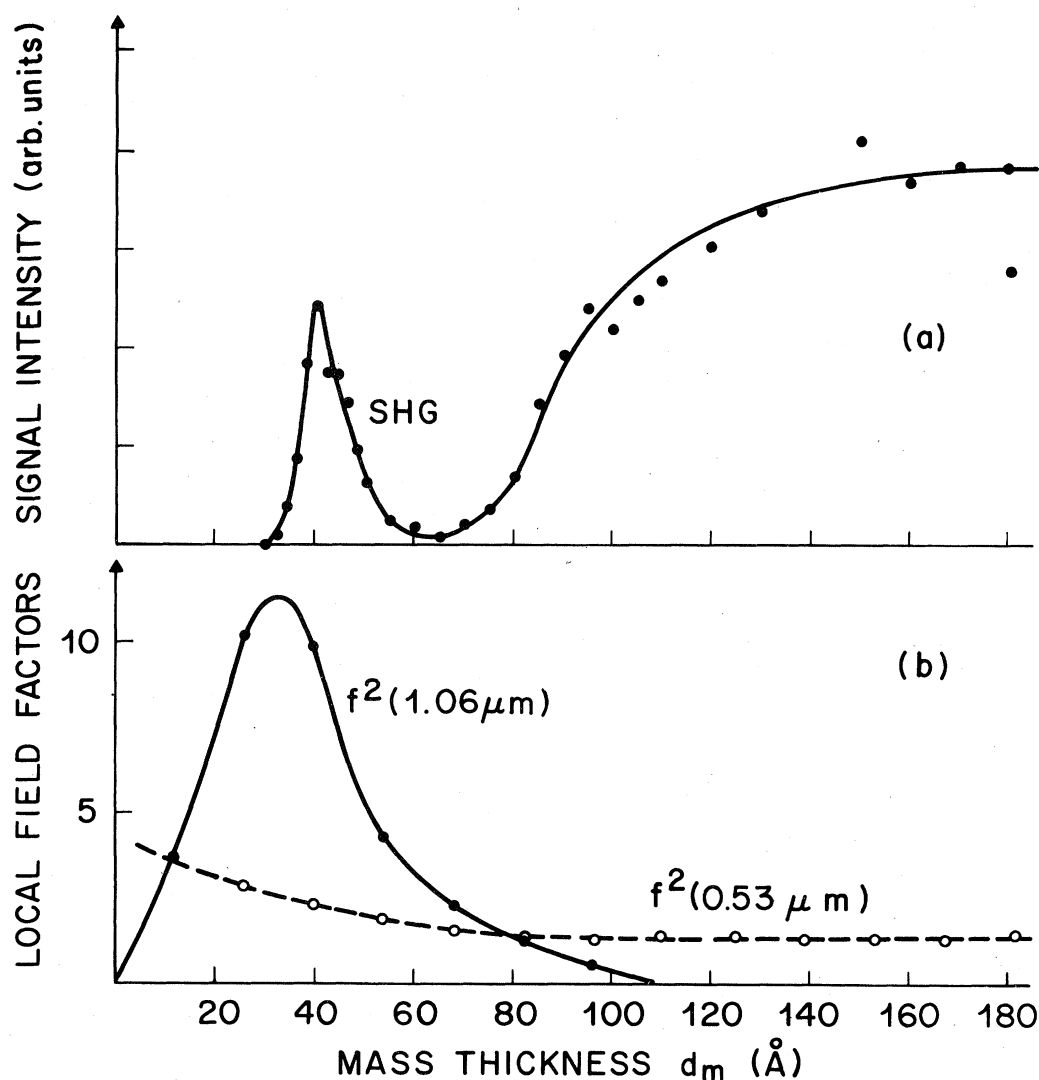


FIG. 2. SHG from Au island films as a function of mass thickness  $d_m$ . (a) Second-harmonic intensity excited at  $1.06 \mu\text{m}$ . (b) Local field enhancement factors  $|f|^2$  at  $1.06 \mu\text{m}$  (solid circles) and  $0.53 \mu\text{m}$  (open circles).

local field factors  $f(\omega_1)$  and  $f(2\omega_1)$  in Eq. (3), by measuring the effective dielectric constant  $\epsilon_{\text{eff}}(\omega)$  of the films. It is related to the polarization  $P$  of the metal particles by the equation

$$P = \frac{\epsilon_{\text{eff}}(\omega) - 1}{4\pi} E_0. \quad (4)$$

$P$  can be calculated in terms of the fields  $E_{\text{in}} = f(\omega)E_0$  inside the particles,

$$P = q \frac{\epsilon(\omega) - 1}{4\pi} E_{\text{in}}, \quad (5)$$

where  $q$  is the fractional volume occupied by the particles. Combining Eqs. (4) and (5) with the explicit expression for  $f(\omega)$ , Eq. (1), one obtains the desired relationship

$$\text{Im}\epsilon_{\text{eff}}(\omega) = q |f(\omega_i, d_m)|^2 \text{Im}\epsilon(\omega). \quad (6)$$

$\text{Im}\epsilon_{\text{eff}}(\omega)$  represents the loss of the film and is therefore related to its absorption. Wolter<sup>28</sup> has indicated how  $\text{Im}\epsilon_{\text{eff}}(\omega)$  can be obtained from measurements of the transmission  $T$  and reflection  $R$  of thin films at normal incidence, e.g., for the beam entering from the substrate side,

$$\text{Im}\epsilon_{\text{eff}}(\omega_i, d_m) = \frac{q \lambda_i}{2\pi d_m} \frac{A(\omega_i, d_m)}{T(\omega_i, d_m)}, \quad (7)$$

with the absorption calculated as  $A = 1 - R - T$ .

Equations (6) and (7) are used to derive the local field factors  $|f|^2$  from our measurements of the optical properties. In Figs. 1(b) and 2(b), we have plotted the results both at the fundamental and at the SH frequency. For Ag, the plasmon resonance<sup>7,8</sup> is shifted to  $\lambda = 5320 \text{ \AA}$  at  $d_m \approx 27 \text{ \AA}$ ; on the sapphire substrates used in the present study this value is observed at a smaller mass thickness as compared to glass substrates.<sup>7</sup> The local field factor for the fundamental shows a peak at  $d_m \approx 60 \text{ \AA}$ . The maximum of the SH intensity at  $d_m \approx 36 \text{ \AA}$  occurs between these two values, as anticipated from Eq. (3).

As a further independent test of our interpretation, we adsorbed HCN on identically prepared Ag wedges and performed surface-enhanced Raman scattering experiments as a function of mass thickness,<sup>7</sup> using an excitation wavelength of  $5145 \text{ \AA}$ . The results show a peak at  $d_m \approx 40 \text{ \AA}$ , again shifted to smaller  $d_m$  as compared to glass where it occurs at  $60 \text{ \AA}$ .<sup>7</sup>

For Au, the local field factor at  $1.06 \mu\text{m}$  reaches its peak value for  $d_m \approx 33 \text{ \AA}$ , while  $|f(2\omega_1)|^2$  is represented by a monotonically decreasing function. The peak in SHG is found at  $d_m \approx 40 \text{ \AA}$ , and is

thus clearly due to the resonant enhancement of the fundamental. In this respect the Au films are distinct from the Ag islands where the enhancement is mainly due to the plasmon at the second-harmonic frequency. The smaller size of the Au plasmon resonance peak is qualitatively understood in terms of the higher dielectric losses of this metal.

As the mass thickness is increased beyond the particle plasmon peak, the resonance condition is no longer fulfilled, and the SH intensity drops by a factor of  $\geq 50$ , for both Ag and Au island films. However, for  $d_m \geq 100 \text{ \AA}$  the signal increases again, as is seen in Figs 1(a) and 2(a). This rise is due to the onset of a different SHG enhancement mechanism, which will be discussed in the following section.

### C. SHG signals at high mass thickness

Sizable SHG signals are observed, both for Ag and Au, in the mass thickness range  $d_m \geq 100 \text{ \AA}$ , where the metal islands have coalesced into a continuous film. We attribute this effect to residual surface roughness, leading to the launching of non-localized surface plasmons by the beam incident at  $50^\circ$  to the surface normal. Simon *et al.*<sup>29</sup> have measured SHG from a  $560\text{-\AA}$  Ag film excited at  $\lambda = 6943 \text{ \AA}$ , and observed an enhancement by a factor of 30 when prism coupling into the extended surface plasmon of a smooth metal surface, with a calculated enhancement of 150. Even larger enhancements have been seen by Chen *et al.*<sup>30</sup> using counterpropagating surface plasmons. In this context, the following points are worth noting. (i) Scanning electron microscope (SEM) pictures of our films at high mass thickness show considerable surface corrugations, possibly due to inhomogeneities or microscratches on the sapphire substrate. (ii) A control experiment was performed on a sapphire slide with two regions of constant Ag mass thickness ( $700$  and  $2500 \text{ \AA}$ ), with the  $1.06\text{-}\mu\text{m}$  beam entering from the sapphire side. A  $700\text{-\AA}$  film is suitable to launch surface plasmons on the Ag-air interface when entering from the backside of the film, provided that phase matching is achieved due to surface irregularities at the proper angle. Indeed we observe a relatively high Sh signal ( $I_{2\omega}/I_\omega^2 = 5 \times 10^{-19} \text{ cm}^2 \text{ W}^{-1}$ ) with large variations as the beam is translated across the surface. For  $d_m = 2500 \text{ \AA}$ , only surface plasmons on the sapphire-silver interface can be excited. The SH intensity is observed to drop by a factor of  $\sim 2$ , with much smaller excursions from the average value.

To summarize our interpretation of Fig. 1(a), we are observing a particle plasmon resonance at  $d_m \approx 36 \text{ \AA}$ , corresponding to an enhancement of  $\sim 10^3$ . For higher mass thicknesses, the enhancement first drops sharply, and then rises again as the particles coalesce and the launching of extended surface plasmons becomes effective, leading to a plateau enhancement of  $\sim 10^2$ .

The peak enhancement of  $\sim 10^3$  was calculated based on the SHG conversion efficiency from a smooth Ag surface reported by Bloembergen.<sup>18,23</sup> Our result is consistent with the recent measurements by Chen *et al.*<sup>15</sup> who observed an enhancement of  $10^4$  on electrochemically roughened silver. A point of concern, however, is the report of considerably larger SHG signals from thick Ag films by Sonnenberg and Hefner.<sup>19</sup> They determined  $I_{2\omega}/I_\omega^2 = 9 \times 10^{-19} \text{ cm}^2 \text{ W}^{-1}$  at  $\lambda = 6943 \text{ \AA}$  for Ag films independent of thickness in the range 150–23 000 Å, a number 70 times larger than the corresponding result by Bloembergen *et al.*<sup>18,23</sup> If the result of Sonnenberg and Hefner is representative for a perfectly smooth silver surface, extrapolation to  $1.06 \mu\text{m}$  would imply that our peak SHG signal only corresponds to an enhancement of about 10.

It is interesting to compare the SHG enhancements ( $\sim 10^3$ ) with SERS where enhancements are typically  $\sim 10^6$ . The origin of this difference is seen by comparing Eqs. (2) and (3). Firstly since  $|\epsilon(\omega)|$  is large for coinage metals in the visible frequency range, the amplified incident field outside the particle surface (polarizing the Raman molecule) is considerably larger than the field inside the surface (relevant for SHG). Secondly, the Raman frequency shifts are relatively small such that for SERS the simultaneous enhancement of incident and scattered fields is possible, with the intensity roughly proportional to  $f^4(\omega_0)$ . In SHG we were presently enhancing only one frequency, such that in the case of Ag the intensity was mainly enhanced by  $f^2(0.53 \mu\text{m})$ . The same reasoning also explains why *no* SERS signal is observed for high mass thicknesses<sup>7</sup> in contrast to SHG. From Fig. 1(b) we see that  $f^2(0.53 \mu\text{m})$  decreases by a factor of 10 from  $d_m = 25 \text{ \AA}$  to  $d_m = 100 \text{ \AA}$ . Squaring this ratio we predict that the Raman signal at high mass thickness will be 100 times smaller than its peak value at  $d_m \approx 40 \text{ \AA}$ , which is below our detection sensitivity.

Substantial SHG signals are observed from high mass thickness Au films, as shown in Fig. 2(a). [Note that the vertical scale is expanded by a factor of 2 as compared to Fig. 1(a).] We attribute these

signals to the same mechanism as for the Ag films, i.e., the launching of extended surface plasmons. SEM pictures of the coalesced Au island films at  $d_m \approx 180 \text{ \AA}$  also show grooves and corrugations with typical distances of  $0.5 - 1 \mu\text{m}$ , which are suitable to promote the excitation of extended plasmons. Why this mechanism is, in the case of Au, more effective than the particle plasmon SHG enhancement (at  $d_m \approx 40 \text{ \AA}$ ), is presently not yet understood.

#### IV. SHG FROM MICROLITHOGRAPHIC SILVER PARTICLE SURFACES

A second set of experiments employed an array of uniformly sized and shaped Ag spheroids as the nonlinear medium. The technique for producing a square array of slightly conical  $\text{SiO}_2$  posts on a silicon substrate has been described elsewhere.<sup>8</sup> Ellipsoidal particles of  $1000 \times 1000 \times 3000 \text{ \AA}^3$  dimensions were attached to the tops of the posts by evaporating Ag at an angle of  $68^\circ$  to the surface normal. A previous study<sup>8</sup> of Raman scattering from a monolayer of CN adsorbed on these particles had shown a maximum of surface enhancement for an excitation wavelength of  $5300 \text{ \AA}$ . We therefore expected SHG to be enhanced due to the factor  $f(2\omega_1)$  in Eq. (3). With identical experimental setup, we indeed observe SH signals on the specularly reflected beam. The magnitude of the signal depends strongly on the angle of incidence, with a maximum at  $\theta_{\text{in}} \approx 50^\circ$ . This maximum value corresponds to  $I_{2\omega}/I_\omega^2 \approx 1.2 \times 10^{-17} \text{ cm}^2 \text{ W}^{-1}$ , i.e.,  $\approx 5$  times the peak value from Ag island films. This larger enhancement, in spite of a lower packing density for the lithographic particle surfaces [ $q \approx 0.05$  in Eq. (5)], is presumably due to the high uniformity in shape,<sup>8</sup> such that practically all particles are resonant with the SH frequency.

From the regularity of the array of posts supporting the Ag particles, and the coherent nature of SHG, one anticipates the observation of diffraction effects. Rederiving a grating equation for SHG, one has to take into account that a phase lag of  $\pi$  along the path of an incident beam at the fundamental frequency results in a phase change of  $2\pi$  in the diffracted beam at the second harmonic. This leads to the standard equation

$$d(\sin\theta_{\text{in}} - \sin\theta_{\text{out}}) = m\lambda_2, \quad m = 0, \pm 1, \pm 2, \dots \quad (8)$$

where  $d$  is the groove spacing and  $\lambda_2$  is the wavelength of the second harmonic. For the lattice period  $d = 3150 \text{ \AA}$  employed in our experiment, it

is easily verified that no orders aside from the specular reflection exist for the fundamental beam at  $\lambda_1 = 1.06 \mu\text{m}$ . However, the SHG grating equation, Eq. (8), predicts exactly one nontrivial solution for  $m = 1$ . Using an angle of incidence  $\theta_{\text{in}} = 75^\circ$ , we detected a well-defined beam of SH light back-reflected at  $\theta_{\text{out}} = -45^\circ \pm 2^\circ$ . No fundamental light is diffracted into this direction; the divergence of the beam is comparable to the specularly reflected one. The observed angle agrees with the calculated value  $\theta_{\text{out}} = -47^\circ$ . For this configuration, the SH power is divided approximately equally between the two beams. The particle structure could be blazed, by changing the angle of evaporation, to selectively enhance the SH power in the background-free beam.

We have conducted preliminary experiments for exciting SH at 5145 Å. This experiment and other examples of nonlinear optical studies of metal particle surfaces, including enhanced two-photon luminescence of molecules adsorbed on the island films, will be described in forthcoming publications.

## V. CONCLUSIONS

In summary, we have observed SHG from Ag and Au island films on sapphire substrates, with a

peak enhancement of  $\approx 10^3$  at  $1.06 \mu\text{m}$ . It is interesting to compare our results with a smaller enhancement<sup>31</sup> of SHG by a cavity resonating the second-harmonic light. In our case the enhancement is correlated with the resonant excitation of surface waves on the metal particles.

The particles surfaces employed in the present study were essentially enhancing only one of the frequencies in Eq. (3), the fundamental for Au and the second harmonic for Ag. However, by designing suitably shaped particles it may become possible to simultaneously resonate two or several of the relevant frequencies. In this case enhancements comparable to or larger than in SERS (typically  $10^6$ ) are expected, where both the incident and the reradiated field are amplified by the surface roughness. The potential of separating SH beams from the fundamental, by attaching metal particles to grating-type structures and using the odd grating orders according to Eq. (8), appears to be a possible concept for practical devices.

## ACKNOWLEDGMENTS

The authors would like to thank F. A. Beisser and R. M. Hart for technical assistance.

- 
- <sup>1</sup>M. Fleischman, P. J. Hendra, and A. J. McQuillan, *Chem. Phys. Lett.* **26**, 163 (1974).  
<sup>2</sup>The field was recently reviewed by R. P. van Duyne, in *Chemical and Biochemical Application of Lasers*, edited by C. B. Moore (Academic, New York, 1979), Vol. 4.  
<sup>3</sup>J. R. Kirtley and J. C. Tsang, *Bull. Am Phys. Soc.* **24**, 278 (1979).  
<sup>4</sup>J. G. Bergman, J. P. Heritage, A. Pinczuk, J. M. Worlock, and J. H. McFee, *Chem. Phys. Lett.* **68**, 412 (1979).  
<sup>5</sup>J. E. Rowe, C. V. Shank, D. A. Zwemer, and C. A. Murray, *Phys. Rev. Lett.* **44**, 1770 (1980).  
<sup>6</sup>T. H. Wood and M. V. Klein, *Solid State Commun.* **35**, 263 (1980).  
<sup>7</sup>J. G. Bergman, D. S. Chemla, P. F. Liao, A. M. Glass, A. Pinczuk, R. M. Hart, and D. H. Olson, *Opt. Lett.* **6**, 33 (1981).  
<sup>8</sup>P. F. Liao, J. G. Bergman, D. S. Chemla, A. Wokaun, J. Melngailis, A. M. Hawryluk, and N. P. Economou, *Chem. Phys. Lett.*, in press.  
<sup>9</sup>A. M. Glass, P. F. Liao, J. G. Bergman, and D. H. Olson, *Opt. Lett.* **5**, 368 (1980).  
<sup>10</sup>M. Moskovits, *J. Chem. Phys.* **69**, 4159 (1978).  
<sup>11</sup>E. Burstein, Y. J. Chen, and S. Lundquist, *Bull. Am. Phys. Soc.* **23**, 130 (1978).  
<sup>12</sup>S. L. McCall, P. M. Platzman, and P. A. Wolff, *Phys. Lett. A* **77**, 381 (1980).  
<sup>13</sup>J. I. Gersten and A. Nitzan, *J. Chem. Phys.* **73**, 3023 (1980).  
<sup>14</sup>M. Kerker, D. S. Wang, and H. Chew, *Appl. Opt.* **19**, 4159 (1980).  
<sup>15</sup>C. K. Chen, A. R. B. de Castro, and Y. R. Shen, *Phys. Rev. Lett.* **46**, 145 (1981).  
<sup>16</sup>J. Ducuing and N. Bloembergen, *Phys. Rev. Lett.* **10**, 474 (1963); R. K. Chang, J. Ducuing, and N. Bloembergen, *ibid.* **15**, 415 (1965).  
<sup>17</sup>F. Brown, R. E. Parks, and A. M. Sleeper, *Phys. Rev. Lett.* **14**, 1029 (1965); F. Brown and R. E. Parks, *ibid.* **16**, 507 (1966).  
<sup>18</sup>N. Bloembergen, R. K. Chang, and C. H. Lee, *Phys. Rev. Lett.* **16**, 986 (1966).  
<sup>19</sup>H. Sonnenberg and H. Heffner, *J. Opt. Soc. Am.* **58**, 209 (1968).  
<sup>20</sup>C. C. Wang and A. N. Duminski, *Phys. Rev. Lett.* **20**, 668 (1968).  
<sup>21</sup>N. Bloembergen and S. Pershan, *Phys. Rev.* **128**, 606 (1962).  
<sup>22</sup>S. S. Jha, *Phys. Rev.* **140**, A2020 (1965); S. S. Jha and C. S. Warke, *ibid.* **153**, 751 (1967).  
<sup>23</sup>N. Bloembergen, R. K. Chang, S. S. Jha, and C. H. Lee, *Phys. Rev.* **174**, 813 (1968).  
<sup>24</sup>J. Rudnick and E. A. Stern, *Phys. Rev. B* **14**, 4274 (1971).  
<sup>25</sup>E. C. Stoner, *Philos. Mag.* **36**, 803 (1945).

<sup>26</sup>S. Singh, in *Handbook of Lasers*, edited by R. J. Pressley (CRC, Cleveland, 1971), p. 499.

<sup>27</sup>F. Brown and M. Matsuoka, Phys. Rev. 185, 985 (1969).

<sup>28</sup>H. Wolter, Z. Phys. 105, 269 (1937).

<sup>29</sup>H. J. Simon, D. E. Mitchell, and J. G. Watson, Phys.

Rev. Lett. 33, 1531 (1974).

<sup>30</sup>C. K. Chen, A. R. B. de Castro, and Y. R. Shen, Opt. Lett. 4, 393 (1979).

<sup>31</sup>A. Ashkin, G. D. Boyd, and J. M. Dziedzic, IEEE J. Quantum Electron. 2, 109 (1966).